JACS
JOURNAL OF THE AMERICAN CHEMICAL SOCIETY
Article
pubs.acs.org/JACS

Self-Recognition of Structurally Identical, Rod-Shaped Macroions with Different Central Metal Atoms during Their Assembly Process

Panchao Yin,[†] Jin Zhang,[‡] Tao Li,[§] Xiaobing Zuo,[§] Jian Hao,[‡] Anna Marie Warner,[†] Soma Chattopadhyay,[⊥,#] Tomohiro Shibata,[⊥,#] Yongge Wei,*[,‡] and Tianbo Liu*[,†,∥]

[†]Department of Chemistry, Lehigh University, Bethlehem, Pennsylvania 18015, United States
[‡]Department of Chemistry, Tsinghua University, Beijing 100084, P.R. China
[§]X-ray Science Division, Advanced Photon Source, Argonne National Laboratory, Argonne, Illinois 60439, United States
[⊥]CSRRI-IIT, MRCAT, Sector 10, Building 433B, Argonne National Laboratory, Argonne, Illinois 60439, United States
[#]Physics Department, Illinois Institute of Technology, Chicago, Illinois 60616, United States
[∥]Department of Polymer Science, The University of Akron, Akron, Ohio 44325, United States

Supporting Information

ABSTRACT: Two rod-shaped macroanions, $((C_4H_9)_4N)_7[Mo_6O_{18}NC(OCH_2)_3XMo_6O_{18}(OCH_2)_3CNMo_6O_{18}]$ (X = Mn^{III} (**1**), Fe^{III} (**2**)), with almost identical charge densities and morphologies except for their different encapsulated central metal atoms were each observed to self-assemble into "blackberry"-type supramolecular structures in their dilute solution, driven by the counterion-mediated attraction. Amazingly, the two macroions remained self-sorted and self-assembled into homogeneous assemblies in their mixed solutions, demonstrating a self-recognition behavior between two highly similar macroions during their assembly process, as confirmed by DLS, SLS, and TEM/EDS analysis. This self-recognition behavior can be explained by the slightly different charge distributions of the macroanions resulting from their different central atoms (confirmed by theoretical DFT calculations and dissociation experiments) and the high activation energy of the slow assembly process, which suppresses the formation of hybrid oligomers at the beginning of the self-assembly process. This work confirms that the long-range counterion-mediated electrostatic attraction is sensitive to the small difference in macroions and consequently offers the possibility for delicate selectivity and preference among different macroions. This phenomenon might be directly related to (and be the important reason for) some recognition behaviors in biological systems.

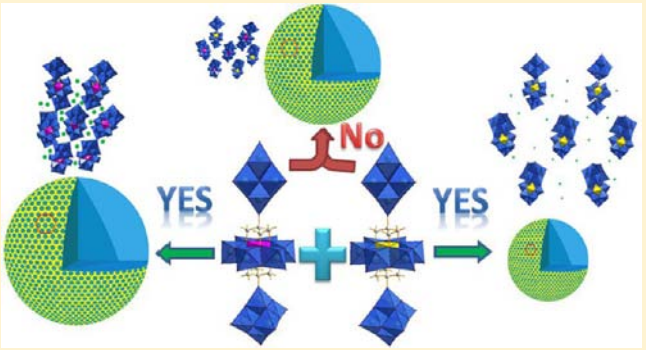

INTRODUCTION

Non-covalent interactions, e.g., hydrogen bonding,[1] $\pi-\pi$ stacking,[2] coordination,[3] static charge interaction,[4] and solvophobic interaction,[5] are responsible for various self-assembly and self-recognition behaviors in physicochemical and biological processes.[6−8] In particular, counterion-mediated like-charge attraction and water-bridged hydrogen bonding were found to play significant roles in the folding, assembly, and recognition behavior of proteins, RNA, and DNA.[9,10] Complex biomolecules rarely function in isolation; hence, a thorough understanding of a biological process is highly dependent upon an examination of assemblies of biomolecules and the interactions driving the assembly process.[11−13] When two different assemblies are in the same solution, they may coexist and remain self-sorted, or they may hybridize.[13,14] Self-recognition phenomena during the self-assembly of biomolecules, in many cases a natural feature of biomacromolecules, contribute to the formation of biomolecular complexes with uniqueness and specific functionality, which are the chemical bases of diverse phenomena such as cell signaling, the immune response, and gene regulatory interaction.[15−18]

An approach to understand the self-recognition processes related to non-covalent interactions is to choose simplified models where only limited types of interactions apply. Nanoscaled polyoxometalate (POM) molecular macroions can be considered as "inorganic polyelectrolytes" composed of negatively charged metal oxide polyhedra with well-defined molecular structures, uniform shapes, tunable charges, and negligible intramolecular charge interaction, which are ideal models for studying the intermolecular interaction of polyelectrolytes.[19−21] Our previous research enables us to understand and control the counterion-mediated attraction between the macroions through the study of the reversible self-assembly of the macroions into stable, hollow, single-layered, "blackberry"-type structures in polar solvents, with the only

Received: January 20, 2013
Published: February 27, 2013

   dx.doi.org/10.1021/ja400656j | J. Am. Chem. Soc. 2013, 135, 4529−4536

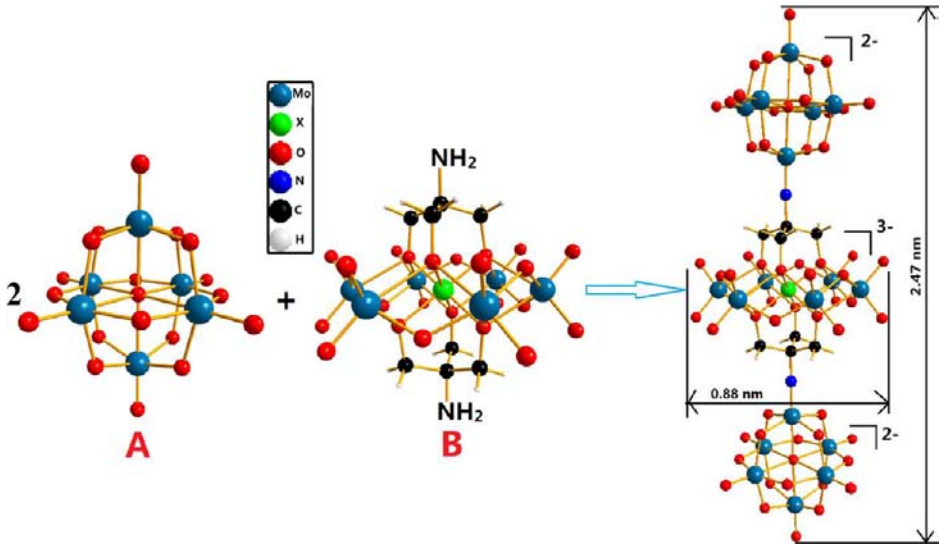

Figure 1. Synthetic procedure for the two molecular rods, using ball−stick representation of the molecular structures of the building blocks and the molecular rods. X, center heteroatom; A, hexamolybdate; B, the ring-shaped Anderson-type molecule.

driving forces being counterion-mediated attraction and hydrogen bonding.[20−28] Such behavior is the result of the counterion−macroion interaction involving moderate counterion association around macroions, a unique phenomenon known only for nanoscaled hydrophilic ions.[20,21,27,29] Very recently, an interesting self-recognition process was observed in the mixed dilute solution of two almost identical, 2.5-nm-size, spherical polyprotic metal oxide-based macroions (abbreviations $\{Mo_{72}Fe_{30}\}$ and $\{Mo_{72}Cr_{30}\}$, respectively).[30] The "Keplerate" clusters $\{Mo_{72}Fe_{30}\}$ and $\{Mo_{72}Cr_{30}\}$ both have 30 $M(H_2O)$ groups coordinated to the non-Mo metal atoms, but different mobilities of their surface hydration layers as well as different degrees of deprotonation. The two types of clusters demonstrate self-recognition by forming two types of homogeneous blackberries instead of mixed ones in their mixed aqueous solution.[30] The charge difference between the two macroions (−7 and −5, respectively) is believed to be the major reason, suggesting that the long-range, delicate electrostatic interaction is essential and critical for self-recognition behavior.[30] In contrast, the assemblies with close-contact interactions (e.g., hydrophobic interactions) cannot achieve this recognition; e.g., different types of surfactants usually form hybrid micelles.[31−33]

It is interesting to notice that simple inorganic macroions can demonstrate the level of self-recognition usually believed to exist only among biomolecules.[18] While the delicate electrostatic interaction is attributed to this behavior, it is critical to test the universality of this behavior among various macroions and, more importantly, to push the limit by studying highly similar mixed macroions. Herein, we report the study of a mixture of two highly charged rod-shaped macroions with almost identical structures and charge densities, differing only in their encapsulated central metal atoms. Time-resolved static and dynamic light scattering, transmission electron microscopy, and energy-dispersive X-ray spectroscopy were utilized to analyze the self-recognition behavior between the two molecular rods. Density functional theory calculation and kinetic monitoring of the disassembly process of the formed blackberry structures in the individual solutions of the two molecular rods and their mixture solution, respectively, were combined to uncover the mechanism for their self-recognition behavior.

EXPERIMENTAL SECTION

Static Light Scattering (SLS). A commercial Brookhaven Instrument LLS spectrometer equipped with a solid-state laser operating at 532 nm was used for measurement of both SLS and DLS. SLS experiments were performed at scattering angles θ between 20 and 120°, at 2° intervals. However, due to the large fluctuations in scattered intensities at low scattering angles, we removed the data from 20 to 40° in the final analysis. Derived from the Rayleigh−Gans−Debye equation,[34] a partial Zimm plot was used to analyze the SLS data to obtain the radius of gyration, R_g. The partial Zimm plot stems from the following approximate formula: $1/I = C(1 + R_g^2q^2/3)$. Here R_g is determined from the slope and intercept of a plot of $1/I$ vs q^2.

Dynamic Light Scattering (DLS). DLS measures the intensity−intensity time correlation function by means of a BI-9000AT multichannel digital correlator. The field correlation function $|g^{(1)}(\tau)|$ was analyzed by the constrained regularized CONTIN method[35] to yield information on the distribution of the characteristic line width Γ from $|g^{(1)}(\tau)| = \int G(\Gamma)\, e^{-\Gamma\tau}\, d\Gamma$.The normalized distribution function of the characteristic line width, $G(\Gamma)$, so obtained, can be used to determine an average apparent translational diffusion coefficient, $D_{app} = \Gamma/q^2$. The hydrodynamic radius R_h is related to D via the Stokes−Einstein equation, $R_h = kT/6\pi\eta D$, where k is the Boltzmann constant and η the viscosity of the solvent at temperature T. From DLS measurements, we can obtain the particle-size distribution in solution from a plot of $\Gamma G(\Gamma)$ versus R_h. The R_h of the particles is obtained by extrapolating $R_{h,app}$ to zero scattering angle.

Transmission Electron Microscopy (TEM) and Energy-Dispersive X-ray Spectroscopy (EDS). The TEM images were taken on a JEOL JEM-2000 electron microscope operated at 200 kV with EDS attachment (Oxford). Samples for the TEM analysis were prepared by dropping a small volume of the solution sample onto a carbon film on a copper grid.

1D NMR and 2D Diffusion Ordered ^{1}H NMR Spectroscopy (DOSY). All the NMR spectra were recorded on a Bruker Avance 500 spectrometer equipped with a BBO probe at 25 °C. For ^{1}H NMR experiments, 2.0 mg of compound **1** and 1.1 mg of TBA*I were each dissolved in 1 mL of acetone-d_6.

DOSY was performed on a Bruker 500 MHz spectrometer with the magnetic field gradient g varying from 0 to 32 G/cm in 16−32 steps. The length of the gradient, d, was from 6000 to 8000 ms, and the time interval between two pulsed gradients, D, was from 0.1 to 0.15 s. All spectra were taken at room temperature. After the data collection,

dx.doi.org/10.1021/ja400656j | J. Am. Chem. Soc. 2013, 135, 4529−4536

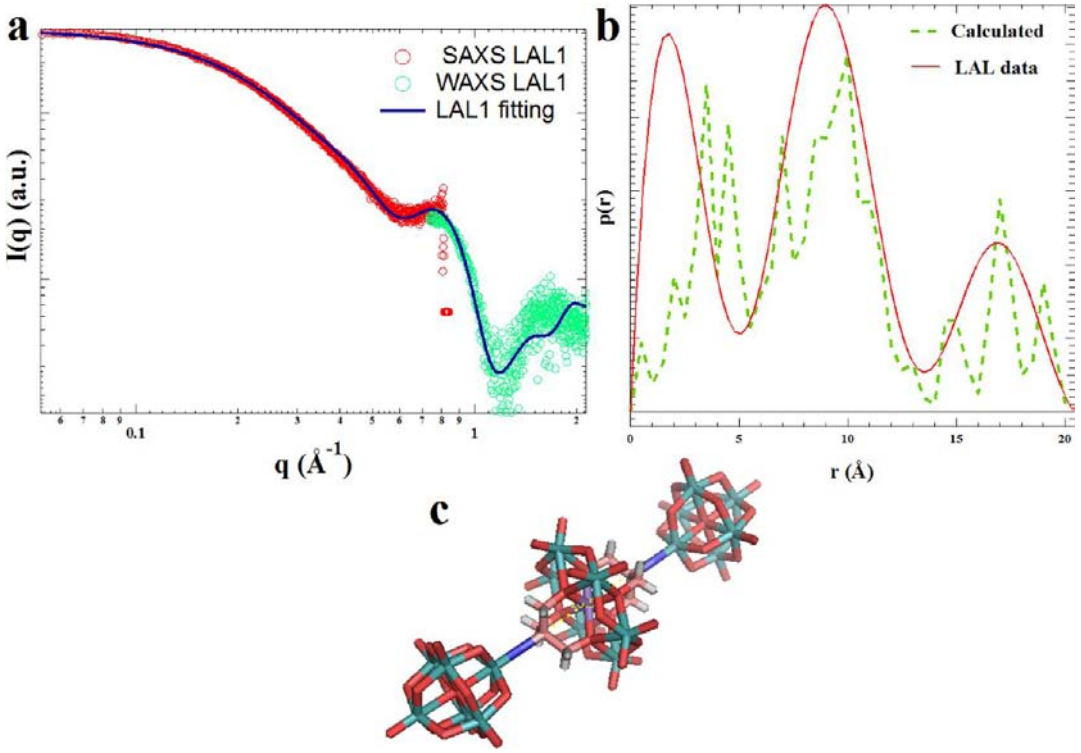

Figure 2. (a) Superimposition of experimental solution small-angle (red circles) and wide-angle (green circles) X-ray scattering curves of **1** in acetonitrile (2 mg/mL) and simulated scattering curve (in blue) using the program SolX with the molecular model (c). (b) PDDF of **1** in its acetonitrile solution (red curve) obtained using the program GNOM, and PDDF calculated (green curve) from the molecular model (c) using SolX. The broadening features in the PDDF obtained from GNOM could arise from the configurational ensemble in solution due to the free rotation of the Mo−N−C bond. (c) The build molecular model for experimental data fitting.

FIDs were processed and analyzed with the NMR software TopSpin 2.0 provided by Bruker. Both T1/T2 relaxation and CONTIN methods were used to fit the raw data. The observed proton signal I in a standard DOSY spectrum is expressed through eq 1:

$$I = I_0 \exp\left[-(2\pi\gamma\delta)^2\left(\Delta - \frac{\delta}{3}\right)Dg^2\right] \quad (1)$$

where I_0 is the reference intensity and γ the gyromagnetic ratio of the proton. If only one diffusive component exists in the solution, a straight line will occur in a plot of $\ln(I/I_0)$ versus g^2, and the apparent diffusion coefficient D can be calculated from the slope using linear regression analysis.

Small-Angle X-ray Scattering (SAXS). The SAXS experiments were performed at station 12-ID-B with X-ray energy of 12 keV at the Advanced Photon Source of the Argonne National Laboratory. The sample-to-detector distance was about 2 m. A 2D CCD detector was used to acquire images with typical exposure times around 1.0 s.

RESULTS AND DISCUSSION

Macroionic Features and Stability of the Molecular Rods in Solution. Two molecular rods, $((C_4H_9)_4N)_7[Mo_6O_{18}NC(OCH_2)_3XMo_6O_{18}(OCH_2)_3CNMo_6O_{18}]$ (X = Mn^{III} (**1**), Fe^{III} (**2**)), were synthesized and fully characterized in previous literature.[36] These two compounds were synthesized by covalently linking two super-octahedron-shaped hexamolybdates (A) onto the two sides of a ring-shaped Anderson-type POM (B) (Figure 1). Basically, the two molecular rods are identical except that the center heteroatom of the ring-like molecule is different: Mn^{III} for rod **1** and Fe^{III} for rod **2**. Both molecular rods are highly charged (−7) with tetrabutylammonium (TBA) as counterion, and hydrophilic with the surface composed of molybdenum oxide. Due to the non-conjugative nature of the linkage between A and B units, they retain their original charges of −2 and −3, respectively (Figure 1). Molecular rods **1** and **2** have identical lengths and diameters of ∼2.77 and 0.88 nm, respectively. The actual structures of the molecular rods in solution (acetonitrile) have been investigated through solution SAXS with a spatial resolution of 2.9 Å.[37] The two molecular rods show identical SAXS curves (Figures 2a and S7 (Supporting Information)), suggesting that they have identical molecular structure in solution state. The calculated SAXS profile for the rod-shaped molecular model fits well with the experimental data of **1**, indicating that the rod shape remains when the crystals of **1** dissolve in acetonitrile (Figure 2a).[38] The radius of gyration of the molecule, R_g = 0.73 nm, is calculated from the small-angle region of SAXS using the Guinier equation. Further exploration of the scattering data with the program GNOM generates pair distance distribution functions (PDDFs) in real space, $p(r)$.[39] The PDDFs exhibit the features of rod-shaped molecular triads, where the first peak centered at ∼0.25 nm describes the intra-subunit (A or B) atom-pair distances, while the second peak at ∼0.90 nm and the third peak at ∼1.70 nm represent the separations of A to B and A to A, respectively (Figure 2b,c). Time-resolved solution X-ray scattering studies and scattering measurements on aged samples suggest that the molecular rods are quite stable, at least for 2 months (Figure S8). As a general feature of the solution physical chemistry of macroions, the ion-pairing of the molecular rods with the counterion, TBA, was investigated by ^{1}H NMR and 2D diffusion-ordered ^{1}H NMR spectroscopy (DOSY).[40] The four-proton peaks of TBA in acetone-d_6 solution of **1** were much broader than in acetone-d_6 solution of tetrabutylammonium iodide (TBA*I), suggesting

dx.doi.org/10.1021/ja400656j | J. Am. Chem. Soc. 2013, 135, 4529−4536

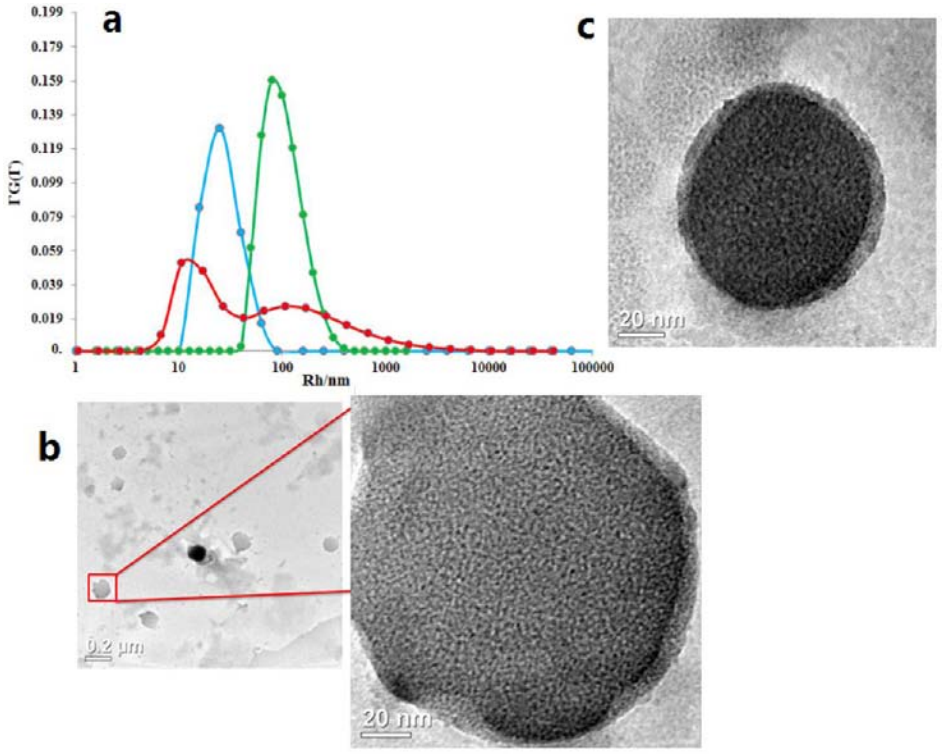

Figure 3. (a) CONTIN analysis of DLS results of the solutions of **1** (green dots), **2** (blue dots), and their mixture (red dots). (b,c) TEM images of assemblies in the solutions of **1** and **2**, respectively.

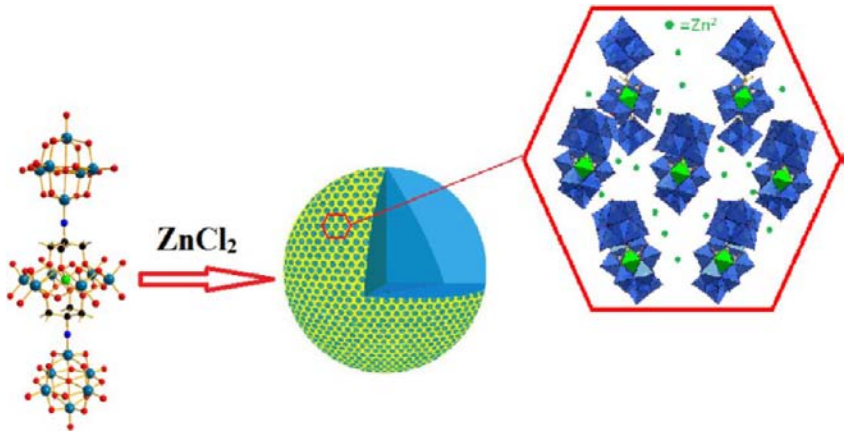

Figure 4. Self-assembly of molecular rods into blackberry structures (polyhedra code: blue, MoO_6 or MoO_5N; green, MnO_6 or FeO_6).

possible strong association of TBAs with large structures in **1**'s acetone solution (Figure S9). DOSY results indicated that TBAs in the solution of **1** diffuse much more slowly (diffusion coefficient $D = 2.8 \times 10^{-9}$ m^2/s) than the "free" TBAs in TBA*I solution ($D = 4.4 \times 10^{-9}$ m^2/s), suggesting strong association of TBAs with the molecular rods (Table S1). The charge density of the molecular rods is -1.06 e/nm^2, which is higher than the range that might be expected for the counterion-mediated static charge-regulated self-assembly of macroions into blackberries.

Self-Assembly of the Molecular Rods into Blackberries. The two rod-like molecules are quite soluble in acetonitrile but do not self-assemble into large supramolecular structures in dilute solution with the bulky and hydrophobic TBA counterions, due to their high surface charge density. Adding $ZnCl_2$ to their acetonitrile solutions can trigger the self-assembly process, since Zn^{2+} ions are more likely to interact with rod-like macroanions than the TBA^+ ions. This leads to stronger counterion-mediated attraction and consequently results in the self-assembly. Time-resolved SLS results indicated that the scattered intensities at 90° scattering angle for both types of rod-like macroionic solutions at room temperature showed a linear increment with time and reached equilibrium at ~40 days (Figure S1). DLS results indicated that the hydrodynamic radii (R_h) of the assemblies in each individual solution of two molecular rods did not change during the whole self-assembly process (Figures S2 and S3). The combination of DLS and SLS suggested that it was the number of the assemblies, not the assembly size, that increased during the self-assembly process. A typical CONTIN analysis from the DLS study of individual solutions of the compounds indicated that R_h of large assemblies showed no angular dependence, with

dx.doi.org/10.1021/ja400656j | J. Am. Chem. Soc. 2013, 135, 4529−4536

narrow distribution and average values of 80 ± 4 and 27 ± 2 nm (Figure 3a), respectively, for the solutions of **1** and **2**. SLS study analyzed by Zimm plot indicated that the assemblies had average R_g = 76 ± 4 and 30 ± 2 nm, respectively. The ratio of $R_h/R_g \approx 1.0$ suggests a hollow spherical structure for each of the assemblies of **1** and **2**, which is also confirmed by TEM results (Figure 3b,c). The counterion (Zn^{2+})-mediated attraction among the highly charged molecular rods is responsible for the formation of the assemblies (blackberries), which shows some obvious similarities with natural biomacromolecules, such as viral capsid proteins.[41,42] Both the blackberry and spherical viral capsid are nanoscaled single-layer hollow shells, which are quite different from the vesicles of lipid molecules (Figure 4). Moreover, the two assemblies demonstrate similar kinetic features: rate-limiting oligomer formation followed by rapid formation of the large assemblies from the oligomers.[41] The formed blackberry-type structures of **1** and **2** are of obviously different sizes, although the two macroanions are almost identical in both shape and charge. It is believed that the encapsulated central metal ions lead to distortion of the Anderson-type POM framework and therefore affect the charge distribution of unit B. The different charge distributions of the two macroions play a vital role in the binding of added counterion (Zn^{2+}) on the surface of the macroions, which finally determines the size of the assemblies. More details on the mechanism will be discussed in the next section.

Self-Recognition Behavior of the Two Molecular Rods. Impressively, the two inorganic molecular rods show self-recognition behavior by self-assembling into two types of individual blackberry structures instead of mixed ones in their mixed solution. The macroionic shape, surface composition, charge, and counterions are expected to play vital roles in the self-assembly process, based on our previous research.[21] However, for the two molecular rods, all of those factors look identical, making the possible self-recognition challenging and intriguing. It thus provides a good opportunity to explore the extreme conditions required for this phenomenon. A mixed acetonitrile solution of **1** and **2** (1:1 molar ratio, 0.25 mg/mL each) was prepared to study their self-recognition behavior. The resulting two separated modes in the CONTIN analysis of DLS study of the mixed solution indicated the presence of two differently sized large species (Figure 3a). The two peaks, within the error limit of the CONTIN analysis, correspond to those assemblies from the individual solutions containing either molecular rod **1** or **2** with the same concentration and added $ZnCl_2$ amount, indicating that the molecular rods might recognize each other and assemble into their individual homogeneous blackberry structures (Figures 3a and 5).

Additionally, time-resolved SLS results indicated that the two molecular rods self-assembled at similar speeds in their individual acetonitrile solutions with the same rod concentration (0.5 mg/mL, Figure S1), which rules out the possibility that the self-recognition is primarily due to kinetic effects (i.e., that one type of molecular rods assembles faster). Meanwhile, the mixed solution of **1** and **2** (1:1 molar ratio, concentration 0.25 mg/mL each) showed a much slower overall growth in scattered intensity in SLS, i.e., much slower overall self-assembly process than the individual solution of **1** or **2**, which confirms that the molecular rods favor self-sorting in their mixture solution.

The critical evidence for the self-recognition comes from the combination of TEM and EDS studies. The TEM images of the assemblies in the mixed solution indicate that hollow vesicle-like structures with two different sizes coexist (Figure 6a–c), with sizes close to those of the two corresponding homogeneous blackberries assembled from the molecular rods, respectively, confirming the existence of two large species in DLS results on the mixed solution. Moreover, EDS results for the individual blackberries suggested that the dominant metal elements for larger vesicular assemblies (size ~160 nm) and smaller vesicular assemblies (size ~60 nm) are Mn and Fe, respectively, besides Mo and Zn (Figure 6d,e), which confirms that molecules **1** and **2** assembled into the larger and smaller vesicles, respectively. The intensities of Mn or Fe peaks in EDS studies are comparatively weak due to their low concentrations in the compounds/assemblies (molar ratio of Mn/Fe to Mo is 1:18). However, the obvious difference between Fe and Mn signals for each measurement is convincing enough to support the model of self-recognition. To rule out the possibility that the EDS results are random, another 18 vesicular assemblies with different sizes were selected for EDS analysis, which were consistent with the previous results and supported the model of homogeneous blackberry structures (Figure S4).

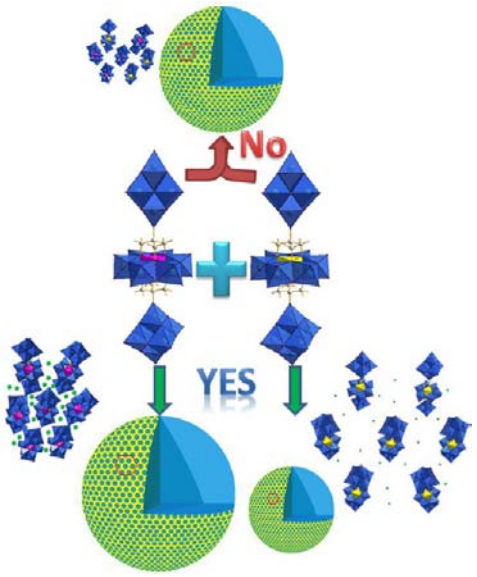

Figure 5. Model of the self-recognition during the self-assembly of two molecular rods in their mixed solution (polyhedra code: blue, MoO_6 or MoO_5N; purple, MnO_6; yellow, FeO_6).

Mechanism of Self-Recognition. Our previous study on the self-assembly of macroions suggests that the formation of oligomers at the beginning of the assembly process is the rate-limiting step with a high activation energy barrier, which enables the preferential formation of self-sorted oligomers in the mixture of **1** and **2** (which might be slightly energetically favored over **1**–**2** mixed dimers).[30] In other words, the formation process is slow compared to the self-assembly of amphiphiles; however, it provides the opportunity for recognition among macroions with minor differences. The heteroatoms encapsulated inside the inorganic molecular rods are the only difference between the two molecules and are expected to lead to the self-recognition behavior (Figures 1 and 5). DFT calculation on Milliken charge distribution indicates that the central Mn atom of molecule **1** is more positively charged than the central Fe atom of molecule **2**, and consequently the perimeter of the planar molecular unit (B) of **1** is more negatively charged than that of **2**, making their net charges still identical for the two macroanions (Tables S2–S4).

dx.doi.org/10.1021/ja400656j | J. Am. Chem. Soc. 2013, 135, 4529–4536

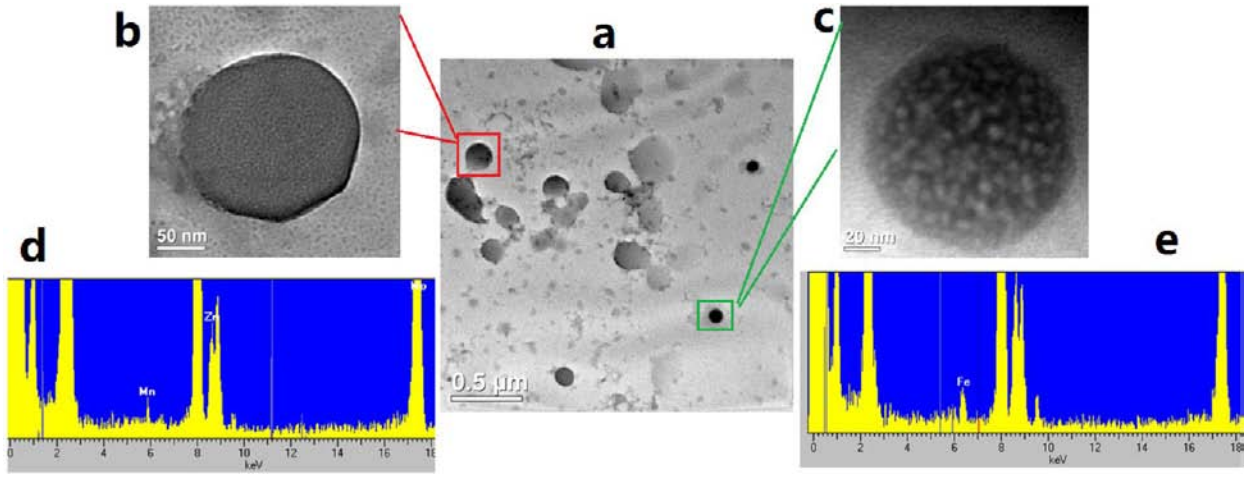

Figure 6. (a) TEM image of the assemblies in the mixed solutions (red rectangle, large assembly; green rectangle, small assembly). (b) Zoom-in image of the large assembly. (c) Zoom-in image of the small assembly. (d) EDS results of the large assembly. (e) EDS results of the small assembly.

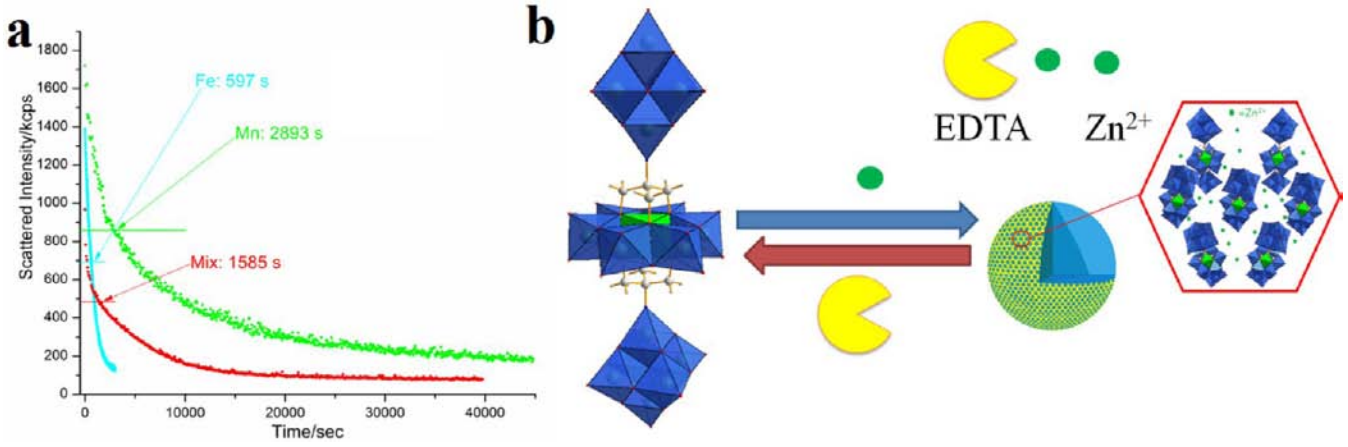

Figure 7. (a) Time-resolved SLS results of the three solutions after adding TBA*EDTA (green, **1**'s solution; blue, **2**'s solution; red, mixture solution). (b) Model of the reversible self-assembly/disassembly process.

Owing to the difference in their charge distributions, **1** is slightly more negative on its surface and able to interact with counterion much more strongly to strengthen the counterion-mediated attraction, which consequently results in the smaller curvature of the assemblies of **1**, e.g., larger sizes for blackberry structures, which has been nicely proved by our experiments (Figure 5).

Due to the anhydrous solution environment, zinc chloride favors binding onto the oxo ligand-enriched surface of the molecular rods, which triggers the blackberry formation for rods **1** and **2** and attributes their difference in charge distribution to the size difference of their assemblies. In contrast to the solvation model of ions in aqueous solution, zinc chloride prefers to directly bind/coordinate onto the surface oxo ligands of POMs since solvent molecules (acetonitrile) are comparatively weak ligands, which can be directly proved by the extended X-ray absorption fine structure experiments (see Supporting Information).[43,44] Thus, the negative charge density of the oxo ligand of the molecular rods, which determines the binding strength of oxo−zinc association, has a significant effect on the blackberry size and the self-recognition behavior. As discussed above, the terminal oxo ligands of **1** carry higher negative charges than those of **2**, which strengthens **1**−$ZnCl_2$ binding and therefore decreases the curvature of assemblies, i.e., increases the blackberry size. Moreover, in the anhydrous acetonitrile solution of the molecular rods, tiny amount of zinc chloride could become partially positively charged by replacement of the chloride ligand with solvent molecule or surface oxo ligand of the clusters, and for that reason we titrated an excess amount of $ZnCl_2$ (molar ratio of $ZnCl_2$ to POM is ∼37) to provide enough counterions for the molecular rods.[43] Binding of Zn complex on the surface of molecular rods can lower the net charge density to a level appropriate for self-assembly. **1** is expected to be more negatively charged on its surface and therefore able to bind more Zn complex than **2**, which lowers the net charge of **1** more and makes its blackberries larger. The ability of **1** to bind strongly with more zinc ions than **2** is further confirmed by the following study, which monitors the disassembly of blackberries in the solutions of the molecular rods after removing $ZnCl_2$.

Dissociation of the Blackberries and Confirmation of the Role of Counterions. Time-resolved SLS results of the above individual acetonitrile solutions of **1** and **2** and their mixed solutions (with $ZnCl_2$ added) at equilibrium indicated that scattered intensity decreased exponentially from values higher than 1000 kcps to ∼100 kcps (scattered intensity for benzene, 113 kcps) when tetrabutylammonium

dx.doi.org/10.1021/ja400656j | J. Am. Chem. Soc. 2013, 135, 4529−4536

ethylenediaminetetraacetate ($(TBA)_4$*EDTA, see Supporting Information; molar ratio of $(TBA)_4$*EDTA to added Zn^{2+} is ~1) was added to each of the solutions, respectively, suggesting the continuous disassembly of the blackberry structures. EDTA is a strong chelating agent that can quickly coordinate with metal ions almost stoichiometrically. In our case, EDTA can extract the Zn^{2+} from the blackberry structures, which will become thermodynamically unstable due to the loss of the counterion-mediated attraction, and consequently disassemble into monomeric molecular rods. The rate-determining step for the disassembly of the blackberry structures is the diffusion of Zn^{2+} from inside shell structures into bulk solution, which is highly dependent on the interaction between molecular rods and Zn^{2+}. The half-life of the disassembly process could be used to estimate the robustness of the macroion−Zn^{2+} interaction and the blackberry structures. In agreement with the DFT calculation results that **1** can interact more strongly with Zn^{2+}, **1**'s solution showed a much longer half-life (2893 s) than that of **2**'s solution (597 s) (Figure 7a). The molecular rods self-assembled in self-sorted ways in their mixed solution and the two types of homogeneous blackberry structures should have different level of robustness according to the above discussions. Therefore, the half-life of the blackberry dissociation in the mixed solution should be longer than that of the solution containing only **2** due to the existence of **1** (and its more robust assemblies), but shorter than that of the solution containing only **1** because of the lower concentration of **1**'s blackberries. This has been fully proved by our experimental results (half-life dissociation for the mixed solution, 1585 s), confirming that the molecular rod **1** can bind zinc complex more strongly than **2** does. Interestingly, the SLS and DLS results of the these three solutions suggested that large assemblies with sizes similar to those of their respective original solutions were observed when $ZnCl_2$ was added to each of the solutions again, which not only confirms the stability of monomers during the self-assembly/disassembly process but also provides us a way to reversibly control the self-assembly/disassembly of macroions in their solutions (Figure 7b and experimental details in Supporting Information).

CONCLUSION

Two types of almost identical macroionic molecular rods, with the only difference being the central atom of their central cluster unit (Mn versus Fe), were observed to self-assemble into hollow spherical blackberry structures and showed self-recognition behavior by assembling into two types of homogeneous blackberries instead of mixed ones in their mixed solution. By controlling the addition and removal of the counterions, Zn^{2+}, the self-assembly/disassembly of the molecular rods can be controlled. This self-recognition achieved between highly similar macroions indicates that the long-range counterion-mediated electrostatic attraction is sensitive to the small difference in macroions and consequently offers the possibility for delicate selectivity and preference among different macroions. This conclusion could be helpful to understand the recognition behavior and self-assembly of biomolecules and direct the design of polyelectrolyte materials.

ASSOCIATED CONTENT

Supporting Information

All experimental details, Tables S1−S5, and Figures S1−S10. This material is available free of charge via the Internet at http://pubs.acs.org.

AUTHOR INFORMATION

Corresponding Author

tliu@uakron.edu; yonggewei@tsinghua.edu.cn

Notes

The authors declare no competing financial interest.

ACKNOWLEDGMENTS

T. Liu acknowledges support from the NSF (CHE1026505) and Lehigh University. T. Li, S. Chattopadhyay, T. Shibata, and X. Zuo are thankful to Dr. Vladislav Zyryanov for designing the sample cells used for measuring the liquid samples and Dr. J. T. Miller of Argonne National Laboratory for fruitful discussions and the use of the Advanced Photon Source. The Advanced Photon Source, an Office of Science User Facility operated for the U.S. Department of Energy (DOE) Office of Science by Argonne National Laboratory, is supported by the U.S. DOE under Contract No. DE-AC02-06CH11357. MRCAT operations are supported by the DOE and the MRCAT member institutions. Y. Wei acknowledges support from NFSC Nos. 21225103 and 20921001, and Tsinghua University Initiative Foundation Research Program No. 20101081771.

REFERENCES

(1) Hanessian, S.; Simard, M.; Roelens, S. *J. Am. Chem. Soc.* **1995**, *117*, 7630.
(2) Salonen, L. M.; Ellermann, M.; Diederich, F. *Angew. Chem., Int. Ed.* **2011**, *50*, 4808.
(3) Langner, A.; Tait, S. L.; Lin, N.; Rajadurai, C.; Ruben, M.; Kern, K. *Proc. Natl. Acad. Sci. U.S.A.* **2007**, *104*, 17927.
(4) Feng, J.; Ruckenstein, E. *J. Chem. Phys.* **2006**, *124*, 124913.
(5) Snyder, P. W.; Mecinović, J.; Moustakas, D. T.; Thomas, S. W.; Harder, M.; Mack, E. T.; Lockett, M. R.; Héroux, A.; Sherman, W.; Whitesides, G. M. *Proc. Natl. Acad. Sci. U.S.A.* **2011**, *108*, 17889.
(6) Lehn, J.-M. *Angew. Chem., Int. Ed.* **1990**, *29*, 1304.
(7) So, C. R.; Kulp, J. L.; Oren, E. E.; Zareie, H.; Tamerler, C.; Evans, J. S.; Sarikaya, M. *ACS Nano* **2009**, *3*, 1525.
(8) Harada, A.; Kobayashi, R.; Takashima, Y.; Hashidzume, A.; Yamaguchi, H. *Nat. Chem.* **2011**, *3*, 34.
(9) Heilman-Miller, S. L.; Thirumalai, D.; Woodson, S. A. *J. Mol. Biol.* **2001**, *306*, 1157.
(10) Roh, J. H.; Behrouzi, R.; Briber, R. M.; Guo, L.; Thirumalai, D.; Woodson, S. A. *Biophys. J.* **2009**, *96*, 575a.
(11) Lehn, J.-M. *Proc. Natl. Acad. Sci. U.S.A.* **2002**, *99*, 4763.
(12) Olson, A. J.; Hu, Y. H. E.; Keinan, E. *Proc. Natl. Acad. Sci. U.S.A.* **2007**, *104*, 20731.
(13) Rebek, J. *Proc. Natl. Acad. Sci. U.S.A.* **2009**, *106*, 10423.
(14) Caulder, D. L.; Raymond, K. N. *Angew. Chem., Int. Ed.* **1997**, *36*, 1440.
(15) Mann, S. *Nature* **1988**, *332*, 119.
(16) Martin, B.; Becourt, C.; Bienvenu, B.; Lucas, B. *Blood* **2006**, *108*, 270.
(17) Misevic, G. N.; Guerardel, Y.; Sumanovski, L. T.; Slomianny, M. C.; Demarty, M.; Ripoll, C.; Karamanos, Y.; Maes, E.; Popescu, O.; Strecker, G. *J. Biol. Chem.* **2004**, *279*, 15579.
(18) *Cellular and Biomolecular Recognition*; Jelinek, R., Ed.; Wiley-VCH: Weinheim, 2009.
(19) Cronin, L.; Muller, A. *Chem. Soc. Rev.* **2012**, *41*, 7333.
(20) Liu, T. *Langmuir* **2010**, *26*, 9202.
(21) Yin, P.; Li, D.; Liu, T. *Chem. Soc. Rev.* **2012**, *41*, 7368.
(22) Kistler, M. L.; Bhatt, A.; Liu, G.; Casa, D.; Liu, T. B. *J. Am. Chem. Soc.* **2007**, *129*, 6453.
(23) Liu, G.; Liu, T. B.; Mal, S. S.; Kortz, U. *J. Am. Chem. Soc.* **2006**, *128*, 10103.
(24) Liu, T. *J. Am. Chem. Soc.* **2003**, *125*, 312.
(25) Liu, T. *J. Am. Chem. Soc.* **2002**, *124*, 10942.

(26) Liu, T.; Imber, B.; Diemann, E.; Liu, G.; Cokleski, K.; Li, H. L.; Chen, Z. Q.; Muller, A. *J. Am. Chem. Soc.* **2006**, *128*, 15914.
(27) Yin, P.; Li, D.; Liu, T. *Isr. J. Chem.* **2011**, *51*, 191.
(28) Liu, T.; Diemann, E.; Li, H.; Dress, A. W. M.; Muller, A. *Nature* **2003**, *426*, 59.
(29) Wang, Y. F.; Weinstock, I. A. *Dalton* **2010**, *39*, 6143.
(30) Liu, T.; Langston, M. L. K.; Li, D.; Pigga, J. M.; Pichon, C.; Todea, A. M.; Müller, A. *Science* **2011**, *331*, 1590.
(31) Tah, B.; Pal, P.; Mahato, M.; Talapatra, G. B. *J. Phys. Chem. B* **2011**, *115*, 8493.
(32) Brito, R. O.; Marques, E. F.; Gomes, P.; Falcão, S.; Söderman, O. *J. Phys. Chem. B* **2006**, *110*, 18158.
(33) Tian, M.; Fan, Y.; Ji, G.; Wang, Y. *Langmuir* **2012**, *28*, 12005.
(34) Hiemenz, P. C.; Rajagopalan, R. *Principles of Colloid and Surface Chemistry*; Marcel Dekker: New York, 1997.
(35) Provencher, S. W. *Comput. Phys. Commun.* **1982**, *27*, 229.
(36) Zhang, J.; Hao, J.; Wei, Y.; Xiao, F.; Yin, P.; Wang, L. *J. Am. Chem. Soc.* **2009**, *132*, 14.
(37) Zhang, R.; Thiyagarajan, P.; Tiede, D. M. *J. Appl. Crystallogr.* **2000**, *33*, 565.
(38) Svergun, D. I.; Koch, M. H. J. *Rep. Prog. Phys.* **2003**, *66*, 1735.
(39) Svergun, D. *J. Appl. Crystallogr.* **1992**, *25*, 495.
(40) Stigter, D. *Biophys. J.* **1995**, *69*, 380.
(41) Zhang, J.; Li, D.; Liu, G.; Glover, K. J.; Liu, T. *J. Am. Chem. Soc.* **2009**, *131*, 15152.
(42) Zlotnick, A.; Aldrich, R.; Johnson, J. M.; Ceres, P.; Young, M. J. *Virology* **2000**, *277*, 450.
(43) Libus, W.; Puchalska, D.; Szuchnicka, T. *J. Phys. Chem.* **1968**, *72*, 2075.
(44) Evans, J. C.; Lo, G. Y. S. *Spectrochim. Acta* **1965**, *21*, 1033.